Inorganic Chemistry

Article

pubs.acs.org/IC

^{1}H and ^{17}O NMR Relaxometric and Computational Study on Macrocyclic Mn(II) Complexes

Gabriele A. Rolla,[†] Carlos Platas-Iglesias,[‡] Mauro Botta,*[,†] Lorenzo Tei,[†] and Lothar Helm[§]

[†]Dipartimento di Scienze e Innovazione Tecnologica, Università del Piemonte Orientale "Amedeo Avogadro", Viale T. Michel 11, 15121, Alessandria, Italy

[‡]Departamento de Química Fundamental, Universidade da Coruña, Campus da Zapateira, Rúa da Fraga 10, 15008 A Coruña, Spain

[§]Laboratoire de Chimie Inorganique et Bioinorganique, Ecole Polytechnique Fédérale de Lausanne, EPFL-BCH, CH-1015 Lausanne, Switzerland

Supporting Information

ABSTRACT: Herein we report a detailed ^{1}H and ^{17}O relaxometric investigation of Mn(II) complexes with cyclen-based ligands such as 2-(1,4,7,10-tetraazacyclododecan-1-yl)acetic acid (DO1A), 2,2′-(1,4,7,10-tetraazacyclododecane-1,4-diyl)-diacetic acid (1,4-DO2A), 2,2′-(1,4,7,10-tetraazacyclododecane-1,7-diyl)diacetic acid (1,7-DO2A), and 2,2′,2″-(1,4,7,10-tetraaza-cyclododecane-1,4,7-triyl)triacetic acid (DO3A). The Mn(II) complex with the heptadentate ligand DO3A does not have inner sphere water molecules ($q = 0$), and therefore, the metal ion is most likely seven-coordinate. The hexadentate DO2A ligand has two isomeric forms: 1,7-DO2A and 1,4-DO2A. The Mn(II) complex with 1,7-DO2A is predominantly six-coordinate ($q = 0$). In aqueous solutions of [Mn(1,4-DO2A)], a species with one coordinated water molecule ($q = 1$) prevails largely, whereas a $q = 0$ form represents only about 10% of the overall population. The Mn(II) complex of the pentadentate ligand DO1A also contains a coordinated water molecule. DFT calculations (B3LYP model) are used to obtain information about the structure of this family of closely related complexes in solution, as well as to determine theoretically the ^{17}O and ^{1}H hyperfine coupling constants responsible for the scalar contribution to ^{17}O and ^{1}H NMR relaxation rates and ^{17}O NMR chemical shifts. These calculations provide ^{17}O $A/\hbar$ values of ca. 40×10^{6} rad s^{-1}, in good agreement with experimental data. The $[Mn(1,4\text{-}DO2A)(H_2O)]$ complex is endowed with a relatively fast water exchange rate ($k_{ex}^{298} = 11.3 \times 10^{8}$ s^{-1}) in comparison to the $[Mn(EDTA)(H_2O)]^{2-}$ analogue ($k_{ex}^{298} = 4.7 \times 10^{8}$ s^{-1}), but about 5 times lower than that of the $[Mn(DO1A)(H_2O)]^{+}$ complex ($k_{ex}^{298} = 60 \times 10^{8}$ s^{-1}). The water exchange rate measured for the latter complex represents the highest water exchange rate ever measured for a Mn(II) complex.

INTRODUCTION

The investigation of stable paramagnetic complexes holds a high level of interest first to contribute to the continuous improvement of fundamental coordination chemistry knowledge and second to implement and develop important applications of these compounds. A remarkable example can be found in the field of magnetic resonance imaging (MRI) contrast agents (CAs). Although fairly recent, the advent of MRI has quickly revolutionized the field of diagnostic imaging over the last four decades, as it has allowed researchers to establish new routine protocols for noninvasive diagnosis. The paramount importance of this application, together with its wide scope and its impact in healthcare, has stimulated thriving investigation activities on inorganic paramagnetic species (mainly Gd(III)-, Mn(II)-, Fe(II)-, and Fe(III)-based compounds), which can act as CAs improving the diagnostic efficiency of MRI.[1,2] The large majority of the metal chelates entered into the clinical practice or investigated during the last 25 years are Gd-based. However, the recent discovery of a disease (nefrogenic systemic fibrosys, NSF) associated with the administration of a Gd(III) chelate based on a bisamide derivative of DTPA to patients affected by advanced renal impairment or subjected to liver transplantation has stimulated the search for safer alternatives to Gd(III) systems.[3] In this context Mn(II) represents an excellent choice as it is an essential element for which living organisms have developed efficient mechanisms for the management of possible excess in organs and tissues. Moreover, complexes of Mn(II) with d^5 high spin configuration present a high effective magnetic moment associated with long electronic relaxation times. This results in an efficient dipolar interaction between the unpaired electron spin of Mn(II) and water-proton nuclear magnetic moment, causing the latter to relax much faster to the equilibrium state leading to enhancement in image contrast. The viability of paramagnetic complexes as efficient CAs is subjected to several conditions;[4] among them are the thermodynamic and kinetic stabilities of the complex (which relate to the safe *in vivo* use of the CA), along with the presence of water molecules directly coordinated to the metal center

Received: December 19, 2012
Published: February 25, 2013

   dx.doi.org/10.1021/ic302785m | *Inorg. Chem.* 2013, 52, 3268−3279

Chart 1. Chemical Structure of the Ligands Investigated in This Work

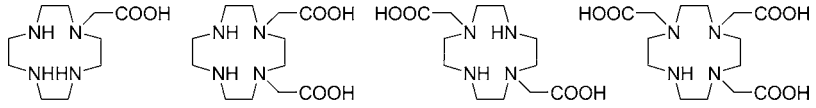

with a proper exchange rate with bulk water (which relates with the contrast enhancement efficiency of the CA).[2b] It is therefore crucial to thoroughly investigate the structural and dynamic properties of paramagnetic complexes intended to be developed into CAs.

In the search for viable applications of Mn(II) complexes in human diagnostic MRI we have previously investigated hexadentate macrocyclic ligands based on a 6-amino-6-methylperhydro-1,4-diazepine scaffold.[5] The relaxivity values (r_{1p}) associated with the corresponding Mn(II) complexes proved surprisingly different from that of the linear hexadentate ligand EDTA. Such difference in relaxivity with the same ligand denticity is unusual for Gd(III) complexes of comparable molecular weights, and recalls attention to the important variability of the critical parameters describing the solution structure of Mn(II) complexes. Aiming at Mn(II) complexes with a good compromise between stability and relaxivity, we focused our attention to cyclen-based ligands and in particular to the two hexadentate isomeric ligands 1,4- and 1,7-DO2A (Chart 1), which have been reported to form thermodynamically stable Mn(II) complexes (log $K_{ML(1,4\text{-}DO2A)}$ = 16.13 and log $K_{ML(1,7\text{-}DO2A)}$ = 14.54).[6]

In fact, only scarce data are available in the literature about these species, existing reports being mainly focused on their thermodynamic stability and solid state X-ray structures,[6] but only marginally on their relaxometric properties. In particular, conflicting data were accounted for [Mn(1,7-DO2A)] which was reported to be six coordinate without inner sphere water molecule (q = 0) but with a relaxivity closer to that of the aqua ion.[7] Moreover, a crystallographic study of [Mn(1,4-DO2A)] showed the formation of a heptacoordinate Mn(II) dimeric complex with two bridging carboxylates.[6] Although the structure of metal complexes in solution can sometimes differ markedly from that observed in the solid state, the hexadentate 1,4-DO2A ligand should leave, in principle, a position open for the coordination of a water molecule in aqueous solution (q = 1). Furthermore, hydration equilibria in the first coordination sphere need to be investigated as they might play an important role as shown for $[Ln(1,7\text{-}DO2A)]^+$ complexes that exhibit average hydration numbers q changing from 3 to 2 across the lanthanide series.[8]

In this Article we report a full ^{1}H and ^{17}O relaxometric study of the whole series of cyclen-based complexes $[Mn(DO1A)]^+$, [Mn(1,4-DO2A)], [Mn(1,7-DO2A)], and $[Mn(DO3A)]^-$ that allowed us to evaluate the parameters that govern the relaxivity associated with these complexes. Additionally, DFT calculations performed at the B3LYP level were used to obtain information on the structure that these complexes adopt in solution, as well as to gain information of the ^{17}O ($A_O/\hbar$) and ^{1}H ($A_H/\hbar$) hyperfine coupling constants (HFCCs) responsible for the scalar contribution to ^{17}O NMR chemical shifts and ^{17}O and ^{1}H relaxation rates. For comparative purposes, we have also performed a reassessment of the parameters governing the relaxivity of $[Mn(EDTA)]^{2-}$ by using new ^{17}O NMR data recorded at 11.5 T, as the measurements reported in the literature were measured on low field instruments.[9]

EXPERIMENTAL AND COMPUTATIONAL SECTION

Materials and Methods. EDTA and $Mn(NO_3)_2$ were obtained from Sigma-Aldrich. Ligands DO1A,[10] 1,4-DO2A,[11] 1,7-DO2A,[12] and DO3A[13] were prepared following literature procedures, and were purified prior to use by precipitation from 6 M aqueous HCl/ethanol mixtures.

General Complexation Procedure To Obtain [Mn(1,4-DO2A)], [Mn(1,7-DO2A)], $[Mn(EDTA)]^{2-}$, $[Mn(DO1A)]^+$, and $[Mn(DO3A)]^-$. Complexation was carried out at pH = 6.0−7.5 by adding aliquots of a standard stock solution of $Mn(NO_3)_2$ (5.9 mM by ICP-MS) to a ca. 6 mM ligand solution and following the linear behavior of the longitudinal relaxation rate of the solution (20 MHz, 298 K) versus the concentration of Mn(II) complex. The absence of free Mn(II) ion was checked by measuring the relaxivity versus pH dependence. By increasing the pH toward the basic region, precipitation of the metal hydroxide occurs with a consequent decrease of relaxivity. The absence of such a relaxivity drop is therefore indicative of the lack of free Mn(II) ions. The exact concentration of the Mn(II) complexes was measured by using the bulk magnetic susceptibility (BMS) shift method.[14] The relaxivity (20 MHz, 298 K, pH = 6.5) was accordingly calculated and resulted to be r_{1p} = 2.1 mM^{-1} s^{-1} for [Mn(1,4-DO2A)], r_{1p} = 1.5 mM^{-1} s^{-1} for [Mn(1,7-DO2A)], r_{1p} = 3.2 mM^{-1} s^{-1} for $[Mn(EDTA)]^{2-}$, r_{1p} = 1.3 mM^{-1} s^{-1} for $[Mn(DO3A)]^-$, and r_{1p} = 2.4 mM^{-1} s^{-1} for $[Mn(DO1A)]^+$ measured at pH = 7.4. Complex solutions were lyophilized and dissolved in water in order to obtain concentrated solutions as required.

^{1}H and ^{17}O NMR Measurements. The water proton longitudinal relaxation rates as a function of the magnetic field strength were measured with a Stelar Spinmaster Spectrometer FFC-2000 (Mede, Pv, Italy) on about 0.5−2.5 mM solutions of the Mn(II) complexes in nondeuterated water. The exact complex concentrations were determined by the BMS shift method and/or by ICP-OES. The reproducibility of the T_1 data was ±5%. The temperature was controlled with a Stelar VTC-91 airflow heater equipped with a calibrated copper−constantan thermocouple (uncertainty of ±0.1 K). The proton $1/T_1$ NMRD profiles were measured on a fast field-cycling Stelar SmartTracer relaxometer over a continuum of magnetic field strengths from 0.00024 to 0.25 T (corresponding to 0.01−10 MHz proton Larmor frequencies). The relaxometer operates under computer control with an absolute uncertainty in $1/T_1$ of ±1%. Additional data points in the range 15−70 MHz were obtained on a Stelar Relaxometer equipped with a Bruker WP80 NMR electromagnet adapted to variable-field measurements (15−80 MHz proton Larmor frequency). Variable-temperature ^{17}O NMR measurements were recorded on a Bruker Avance III spectrometer (11.7 T) equipped with a 5 mm probe and standard temperature control unit. Aqueous solutions of the complexes (10−20 mM) containing 2.0% of the ^{17}O isotope (Cambridge Isotope) were used. The observed transverse relaxation rates were calculated from the signal width at half-height. The ^{17}O NMR experiments were measured on 11.2 mM, 23.9 mM and 14.3 mM solutions of the $[Mn(EDTA)]^{2-}$, [Mn(1,4-DO2A)], and $[Mn(DO1A)]^+$ complexes at pH = 6.5 for $[Mn(EDTA)]^{2-}$and [Mn(1,4-DO2A)] and at pH = 7.8 for $[Mn(DO1A)]^+$.

ESR Spectroscopy. ESR spectra were recorded using a JEOL FA-200 ESR X-band spectrometer with JEOL ES-LC11 flat cell for aqueous samples analysis. ESR spectroscopic analyses were carried out

dx.doi.org/10.1021/ic302785m | Inorg. Chem. 2013, 52, 3268−3279

under the following conditions: temperature 298 K; magnetic field 318 ± 250 mT; field modulation width 0.3 mT; field modulation frequency 100 kHz; time constant 0.01 s; sweep time 2 min; microwave frequency 9.226 GHz, microwave power 10 mW.

Computational Details. All calculations were performed using hybrid DFT with the unrestricted B3LYP exchange-correlation functional,[15,16] and the Gaussian 09 package (Revision A.02).[17] Full geometry optimizations of the $[Mn(1,4\text{-}DO2A)(H_2O)_q]$ (q = 0, 1), $[Mn(1,4\text{-}DO2A)(H_2O)]\cdot nH_2O$ (n = 1 or 4), $[Mn(1,7\text{-}DO2A)]$, $[Mn(DO1A)(H_2O)]^{+}\cdot nH_2O$ (n = 0 or 4), and $[Mn(EDTA)(H_2O)]^{2-}\cdot nH_2O$ (n = 1 or 4) systems were performed in aqueous solution by using the Ahlrich's valence double-ξ basis set with polarization functions (SVP).[18] All systems were modeled in their high-spin configurations ($S = {}^5/_2$), and wave function stability calculations were performed (using the stable keyword in Gaussian 09) to confirm that the calculated wave function corresponded to the ground state. Because geometry optimizations were performed by using an unrestricted model,[19] spin contamination was assessed by comparison of the expected difference between $S(S+1)$ for the assigned spin state ($S = {}^5/_2$) and the actual value of $\langle S^2\rangle$.[20] The results indicate that spin contamination is negligible ($\langle S^2\rangle - S(S+1) < 0.0031$) for all complexes investigated. The stationary points found on the potential energy surfaces as a result of the geometry optimizations have been tested to represent energy minima rather than saddle points via frequency analysis. Solvent effects were evaluated by using the polarizable continuum model (PCM), in which the solute cavity is built as an envelope of spheres centered on atoms or atomic groups with appropriate radii. In particular, we used the integral equation formalism (IEFPCM) variant as implemented in Gaussian 09.[21]

Isotropic ^{17}O and ^{1}H hyperfine coupling constants (HFCCs) in the $[Mn(1,4\text{-}DO2A)(H_2O)]\cdot 4H_2O$, $[Mn(DO1A)(H_2O)]^{+}\cdot 4H_2O$, and $[Mn(EDTA)(H_2O)]^{2-}\cdot 4H_2O$ systems were calculated by using Ahlrich's valence triple-ξ basis set with polarization functions (TZVP)[22] for Mn, while for C, H, N, and O atoms we used the EPR-III basis sets of Barone,[23] which were optimized for the computation of HFCCs by DFT methods. EPR-III is a triple-ζ basis set including diffuse functions, double d-polarizations, and a single set of f-polarization functions, together with an improved s-part to better describe the nuclear region. The hyperfine coupling tensor for the nucleus N consists of three contributions, which are the isotropic Fermi contact (FC) and the anisotropic spin−dipolar contributions and the spin−orbit contribution. In the present work we focus on the isotropic FC contribution (A_{iso}), which is given by[24]

$$A_{iso}(N) = \frac{4\pi}{3S}\beta_e\beta_N g_e g_N \rho^{\alpha-\beta}(R_N) \quad (1)$$

where β_N and β_e are the nuclear and Bohr magnetons, respectively, g_N and g_e are nuclear and free-electron g values, S is the total spin of the system, and $\rho^{\alpha-\beta}$ represents the difference between majority spin (α) and minority spin (β) densities. Thus, A_{iso} is proportional to the value of the spin density at the position of nucleus N, which may be transmitted directly through the bonds by spin delocalization and/or by spin polarization. The hyperfine coupling constants obtained from NMR measurements ($A/\hbar$) are often expressed in rad s^{-1}, and therefore equal $2\pi A_{iso}$ as defined in eq 1.

RESULTS AND DISCUSSION

Assessment of the Hydration State. The increase of the water proton R_1 value, normalized to a 1 mM concentration of the paramagnetic complex, is called relaxivity, r_{1p}, and it represents the efficiency of the metal chelate in catalyzing the solvent relaxation at a given frequency and temperature. The inner-sphere contribution to relaxivity is directly proportional to the number of inner-sphere water molecules (q), and therefore relaxivity values provide information on the hydration level of Mn(II) complexes providing they possess comparable molecular weights and electronic relaxation times. Table 1 shows a comparison of r_{1p} values (20 MHz and 298 K) of the Mn(II) complexes measured in this work with those of several Mn(II) complexes reported in the literature (Chart 2). The data presented in Table 1 indicate that complexes with hexadentate macrocyclic ligands are often associated with lower relaxivities than that of $[Mn(EDTA)]^{2-}$. In some cases, such as for hexadentate AAZ3A derivatives, this has been attributed to the presence of a hydration equilibrium in solution involving q = 1 and q = 0 complex species.[5] As expected, Mn(II) complexes with heptadentate or octadentate ligands lack inner-sphere water molecules, and the observed relaxivity is the result of the outer-sphere contribution only. On the other hand, Mn(II) complexes with pentadentate ligands may possess one or two inner-sphere water molecules but lower stabilities. Thus, the design of Mn(II) complexes for application as MRI CAs is not straightforward, as the same ligand denticity may result in complexes with different hydration numbers depending on different factors such as ligand architecture and steric crowding.

Table 1. Proton Relaxivity (20 MHz and 298 K), Hydration Number, q, and Thermodynamic Stability Constant (log K) for Selected Mn(II) Complexes

	ligand denticity	r_{1p} (mM^{-1} s^{-1})	q	log K_{ML}
[Mn(1,4-DO2A)]	6	2.1[c]	0<q < 1	16.13[6]
[Mn(1,7-DO2A)]	6	1.5[c]	0	14.54[6]
$[Mn(DTPA)]^{3-}$	8	1.5[25,c]	0	
$[Mn(DO3A)]^{-}$	7	1.3[c]	0	19.40[6]
$[Mn(DO3A(BOM)_3)]^{-}$	7	1.6[26]	0	18.80[26]
$[Mn(AAZTA)]^{2-}$	7	1.6[5]	0	14.19[5]
$[Mn(AAZ3MA)]^{-}$	6	1.9[5]	0<q < 1	10.67[5]
$[Mn(MeAAZ3A)]^{-}$	6	2.0[5]	0<q < 1	11.43[5]
$[Mn(AAZ3A)]^{-}$	6	2.5[5]	0<q < 1	11.00[5]
$[Mn(EDTA)]^{2-}$	6	3.3[c]	1	13.88[27]
$[Mn(EDTA(BOM))]^{2-}$	6	3.6[26]	1	
$[Mn(EDTA(BOM)_2)]^{2-}$	6	4.3[26]	1	
[Mn(diPhEDTA)]	6	5.8[28,a]	1	
[Mn(TyrEDTA)]	6	3.7[29]	1	
$[Mn(12\text{-}pyN_4A)]^{+}$	5	2.4[30]	1	11.54[30]
$[Mn(12\text{-}pyN_4C)]$	5	2.8[30]	1	14.06[30]
$[Mn_2(ENOTA)]$	5	3.4[31]	1	24.6[31,b]
$[Mn(9\text{-}aneN_2O\text{-}2P)]^{2-}$	5	5.1[32]	2	10.61[32]
$[Mn(DO1A)]^{+}$	5	2.4[c]	1	

[a]In hepes buffer, 310 K. [b]log K_{M2L}. [c]This work.

Although relaxivity is a complex function of many parameters, when we compare metal complexes of similar structure and molecular weight the r_{1p} value at high frequency (>10 MHz) is roughly proportional to q and thus provides a fairly accurate estimation of the first hydration sphere. The relaxivity of [Mn(1,7-DO2A)] (1.6 mM^{-1} s^{-1} at 20 MHz and 298 K) is quite similar to that of $[Mn(DTPA)]^{3-}$, and typical of a pure "outer-sphere" system (q = 0). Noteworthy, for $[Mn(DO3A)]^{-}$ the relaxivity is even lower (1.3 mM^{-1} s^{-1} at 20 MHz and 298 K); this hints at differences of the outer sphere contribution among cyclic and acyclic q = 0 Mn(II) complexes possibly due to variation in the electronic relaxation behavior. However, the r_{1p} value of [Mn(1,4-DO2A)] (2.1 mM^{-1} s^{-1} at 20 MHz and 298 K) is situated between the limiting relaxivities for complexes with q = 0 (1.5−1.6 mM^{-1} s^{-1}) and q = 1 (2.4−4.3 mM^{-1} s^{-1}) (Table 1 and Figure 1).

The relaxivity data is expected to follow a linear correlation with the molecular weight of the complex at high fields, where

dx.doi.org/10.1021/ic302785m | Inorg. Chem. 2013, 52, 3268−3279

Chart 2. Chemical Structure of the Ligands Reported in Table 1

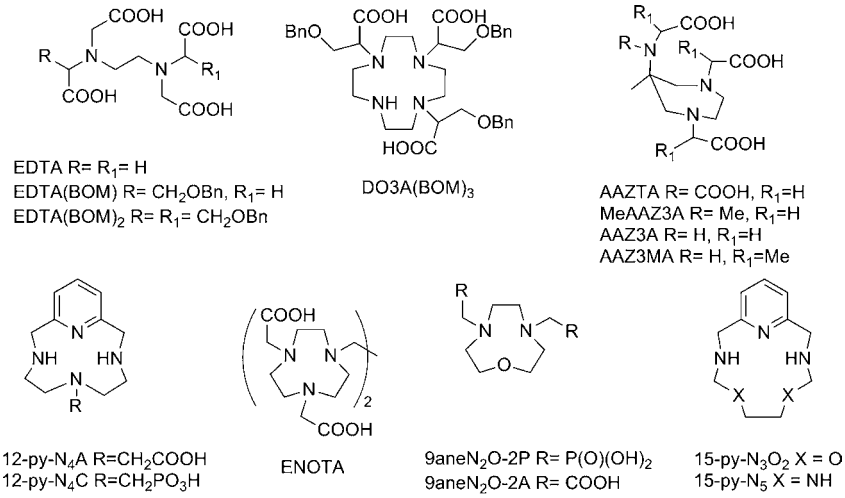

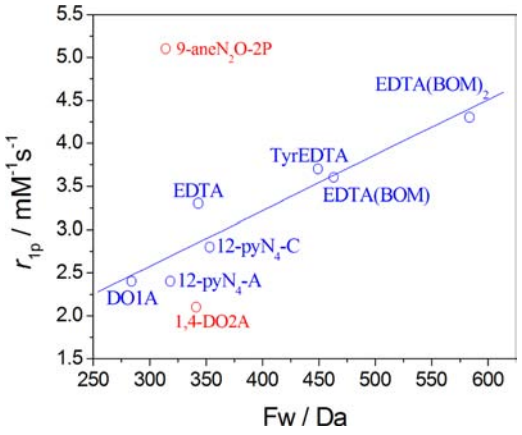

Figure 1. Plot of the relaxivity (20 MHz, 25 °C) of selected Mn(II) complexes with q = 1 as a function of the molecular mass. The linear correlation was calculated with the data given in blue (see text).

the rotational dynamics (τ_R) plays a major role in determining the relaxivity because both the exchange lifetime (τ_M) and the electronic relaxation times are much longer than τ_R. This is indeed the case for the series of mononuclear Mn(II) complexes with q = 1 given in Table 1, with the two evident exceptions of 9-aneN$_2$O-2P and 1,4-DO2A (Figure 1). The former contains two phosphonate groups that are known to be able to promote the formation of a well-defined second hydration sphere that gives an important contribution to r_{1p}.[32] The relaxivity of the second is about 25% lower than the expected value. This effect might be associated with the presence of a hydration equilibrium in solution involving a complex species with one inner-sphere water molecule and a second species with q = 0. This would result in an averaged hydration number of 0 < q < 1, as postulated for the Mn(II) complexes of AAZ3A, MeAAZ3A, and AAZ3MA (Table 1).[5] Another possible explanation for the low relaxivity of [Mn(1,4-DO2A)] could be an unusually long metal bound-water distance (r_{M-H}) associated with an important steric crowding around the water binding site. Noteworthy, the relaxivity of $[Mn(DO1A)]^+$ follows rather well the linear correlation with molecular weight, which points to the presence of one inner-sphere water molecule.

Whereas the relaxivity of [Mn(1,7-DO2A)] remains constant over a broad pH range (5.5−12.0), for [Mn(1,4-DO2A)] a slight increase is observed (≤10%) (Figure 2). This behavior

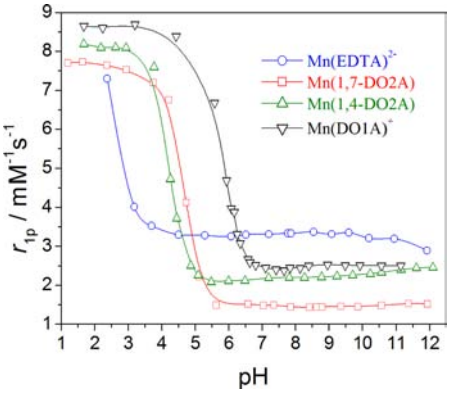

Figure 2. Plot of the relaxivity (20 MHz, 25 °C) of the Mn(II) complexes investigated in this work as a function of pH. The solid lines are simply a guide for the eye.

might be accounted for by an effect of pH on the hydration equilibrium slightly affecting the relative populations of the species with q = 0 and q = 1. On the other hand, both complexes increase strongly their relaxivities at acidic pH (<5) as a consequence of proton assisted metal release. In the case of $[Mn(EDTA)]^{2-}$, proton relaxivity is constant on a broader pH range (4.5−12.0). The proton relaxivity of $[Mn(DO1A)]^+$ increases below pH ∼ 7 due to metal complex dissociation, in line with a lower stability of the complex in comparison to the [Mn(DO2A)] analogues.

Computational Study of Molecular Geometries. Aiming to obtain information on the structure in solution of the Mn(II) complexes reported in this work, we characterized the [Mn(1,4-DO2A)], [Mn(1,7-DO2A)], and $[Mn(DO1A)]^+$ systems by means of density functional theory (DFT) calculations with the B3LYP model. In these calculations we have taken into account solvent effects (water) by using a polarizable continuum model (PCM). Previous investigations on Mn(II) complexes derived from cyclen platforms containing coordinating pendant arms have revealed a *syn* conformation of the ligand in the corresponding complexes, where the pendant arms are oriented to the same side of the macrocyclic unit.[33,34]

dx.doi.org/10.1021/ic302785m | Inorg. Chem. 2013, 52, 3268−3279

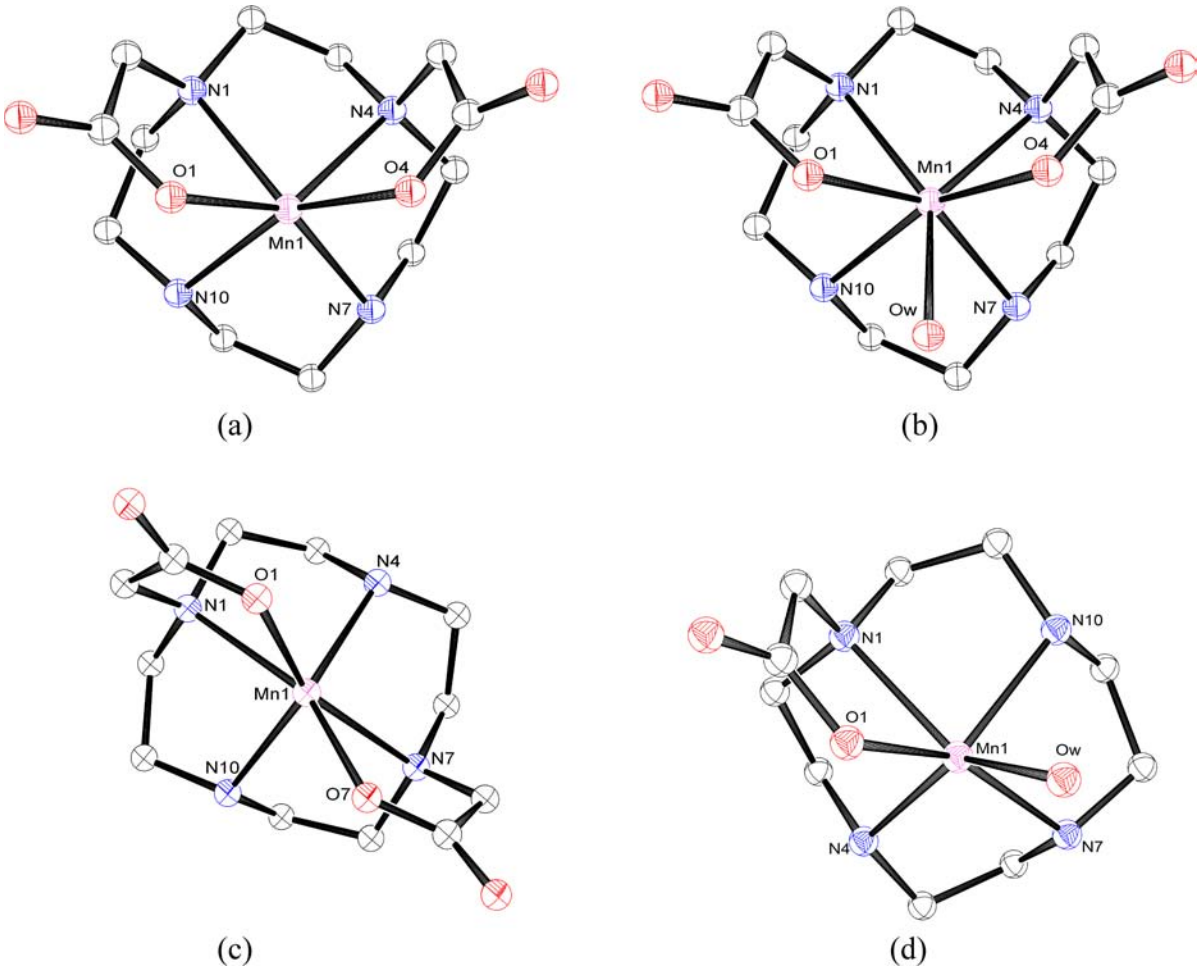

Figure 3. Optimized geometries of the [Mn(1,4-DO2A)] (a), [Mn(1,4-DO2A)(H_2O)] (b), [Mn(1,7-DO2A)] (c), and [Mn(DO1A)(H_2O)]$^+$ (d) systems obtained from DFT calculations performed in aqueous solution by using the B3LYP model. Hydrogen atoms are omitted for simplicity.

Thus, it is reasonable to assume that the complexes of 1,4-DO2A and 1,7-DO2A will adopt a similar structure. A *syn* conformation of the ligand in these complexes implies the occurrence of two helicities: one associated with the layout of the acetate pendant arms (absolute configuration Δ or Λ), and the other to the four five-membered chelate rings formed by the binding of the cyclen (each of them showing absolute configuration δ or λ).[35,36] A careful investigation of the conformational space for these complexes provided a number of local energy minima with different orientations of the acetate groups and the five-membered chelate rings formed upon coordination of the cyclen moiety. The minimum energy conformations obtained for the [Mn(1,4-DO2A)] and [Mn(1,7-DO2A)] complexes are shown in Figure 3, while bond distances of the metal coordination environments are given in Table 2. In the case of the [Mn(1,7-DO2A)] complex the minimum energy conformation corresponds to the $\Lambda(\lambda\lambda\lambda\lambda)$ form [or its enantiomeric pair $\Delta(\delta\delta\delta\delta)$], which possesses a C_2 symmetry. This conformation was previously found in the solid state for the [Mn(H_2DOTA)] complex, where the two acetate pendant arms in positions 4 and 10 are protonated and do not coordinate to the Mn(II) ion.[7] In the lowest energy conformation obtained for [Mn(1,4-DO2A)] the two acetate pendant arms possess different orientations, and therefore the only source of chirality arises from the conformation of the five-membered chelate rings formed upon coordination of the cyclen unit. According to our calculations the four five-membered chelate rings adopt identical conformations [$(\lambda\lambda\lambda\lambda)$ or $(\delta\delta\delta\delta)$]. The optimized geometry of [Mn(1,4-DO2A)] obtained from DFT calculations is very similar to that observed in the solid state for the doubly bridged dimetallic complex [Mn(1,4-DO2A)]$_2$.[6] This gives us confidence in the predictions of the computational procedure used for conformational analysis. The calculated Mn−N bond distances, which range from 2.32 to 2.44 Å, and the Mn−O bond distances, which are between 2.11 and 2.12 Å, are comparable to those usually

Table 2. Bond Distances (Å) of the Mn(II) Coordination Environment Obtained from DFT Calculations (B3LYP) in Water for [Mn(1,7-DO2A)], [Mn(1,4-DO2A)(H_2O)$_q$]·$n$$H_2O$ and [Mn(DO1A)(H_2O)]·$n$$H_2O$

		1,4-DO2A			DO1A	
ligand	1,7-DO2A	q = 0, n = 0	q = 1, n = 0	q = 1, n = 4	n = 0	n = 4
Mn1−N1	2.436	2.392	2.427	2.569	2.374	2.437
Mn1−N4	2.324	2.376	2.398	2.421	2.303	2.297
Mn1−N7	2.436	2.360	2.349	2.341	2.343	2.307
Mn1−N10	2.324	2.371	2.364	2.407	2.317	2.308
Mn1−O1	2.117	2.110	2.157	2.136	2.125	2.197
Mn1−O4		2.122	2.160	2.236		
Mn1−O7	2.117					
Mn1−O_W			2.486	2.373	2.279	2.281

dx.doi.org/10.1021/ic302785m | *Inorg. Chem.* 2013, 52, 3268−3279

found in six-coordinated Mn(II) complexes with polyaminocarboxylate ligands.[37−39]

The coordination polyhedron around the metal ion in [Mn(1,4-DO2A)] can be described as a trigonal prism composed of two nearly parallel (5.4°) triangular faces defined by N1, N10, and O1, and N4, N7, and O4. The mean twist angle[40] of the two triangular faces amounts to 4.9° (ideal value 0°). The metal coordination environment in [Mn(1,7-DO2A)] can be also described as trigonal prismatic, where the two nearly parallel triangular faces (1.1°) are defined by N1, N4, and O1, and N7, N10, and O7. The mean twist angle between these two planes (11.2°) shows a somewhat larger distortion of the coordination polyhedron from a trigonal prism (ideal value 0°) to an octahedron (ideal value 60°). Previous reports suggested that high spin Mn(II) d^5 complexes can accommodate a trigonal prismatic geometry more readily than other electronic configurations.[41]

The relaxivity of the [Mn(1,4-DO2A)] complex may suggest the presence of a hydration equilibrium in aqueous solution involving $q = 1$ and $q = 0$ species. Thus, we performed geometry optimizations on the [Mn(1,4-DO2A)(H_2O)] system. The lowest energy geometry obtained for this system is very similar to that calculated for the $q = 0$ analogue (Figure 3). As expected due to the increasing coordination number, most of the bond distances of the metal coordination environment are longer in the $q = 1$ complex than in the $q = 0$ one (Table 2). The metal coordination environment can be described as monocapped trigonal prismatic, where the inner-sphere water molecule is capping one of the rectangular faces of the polyhedron. The inner-sphere water molecule is bent as a consequence of the hydrogen bonding interaction involving the inner-sphere water molecule and the oxygen atoms of the acetate groups O1 and O4. The distance between the Mn(II) ion and the oxygen atom of the coordinating water molecule (Mn−Ow: 2.486 Å) is ∼0.2 Å longer than those observed in the solid state for monohydrated seven-coordinated Mn(II) complexes.[42,43] This is probably because PCM calculations do not account for specific solute−solvent interactions that are important when dealing with ionic solutes that have concentrated charge densities. To test this hypothesis, we performed DFT calculations on the [Mn(1,4-DO2A)(H_2O)]·$n$$H_2O$ systems ($n = 1$ or 4), which explicitly include second sphere water molecules. The major disadvantage of cluster calculations is that adding extra solvent molecules to the first solvation sphere increases the computational cost. Moreover, the more atoms that are included in the system, the larger the number of degrees of freedom and the higher the number of minimum energy structures.[44] The inclusion of only one second sphere water molecule provokes a dramatic shortening of the Mn−Ow distance to 2.389 Å. This distance is very similar to that calculated for the [Mn(1,4-DO2A)(H_2O)]·4H_2O cluster (2.373 Å). These results indicate that the explicit inclusion of a second sphere hydration shell is required to model the Mn−water interaction in these systems. The distances between the metal ion and the hydrogen atoms of the inner-sphere water molecule in [Mn(1,4-DO2A)(H_2O)]·4H_2O amount to 2.865 and 2.800 Å. Both the Mn−Ow and the Mn···Hw (Hw stands for hydrogen of coordinated H_2O) distances are in good agreement with those normally used for the analysis of the ^{17}O NMR and NMRD data of Mn(II) complexes.

According to our DFT calculations the coordination environment around the metal ion in the [Mn(DO1A)(H_2O)]$^+$ complex is very similar to that predicted for the 1,7-DO2A analogue, with a donor atom of one acetate group being replaced by a coordinated water molecule. The four chelate rings involving ethylenediamine units adopt the same conformation [($\lambda\lambda\lambda\lambda$) or ($\delta\delta\delta\delta$)], resulting in a trigonal prismatic coordination around the metal ion. Contrary to the situation observed for 1,4-DO2A, the Mn−Ow distance is nearly not affected by the inclusion of second-sphere water molecules, which can be attributed to the lower negative charge of the DO1A ligand.

To test the accuracy of the geometries calculated for Mn(II) complexes with DO1A, 1,4-DO2A, and 1,7-DO2A, we have performed analogous calculations on the [Mn(EDTA)(H_2O)]$^{2-}$·$n$$H_2O$ systems ($n = 0$, 4). The calculated bond distances of the metal coordination environment show a good agreement with those observed in the solid state (Table S1, Supporting Information). The Mn−Ow distance calculated for the [Mn(EDTA)(H_2O)]$^{2-}$·4H_2O system (2.309 Å) is ca. 0.06 Å shorter than that obtained for the [Mn(1,4-DO2A)(H_2O)]·4H_2O system, but very close to that calculated for [Mn(DO1A)(H_2O)]$^+$·4H_2O (2.281 Å). The distances between the metal ion and the hydrogen atoms of the inner-sphere water molecule in the EDTA complex are 2.821 and 2.694 Å. Thus, our calculations provide a slightly shorter average metal bound-water distance ($r_{M\text{-}H}$) for the complex of EDTA (2.76 Å) than for the 1,4-DO2A analogue (2.83 Å). For [Mn(DO1A)(H_2O)]$^+$·4H_2O a slightly shorter average $r_{M\text{-}H}$ distance was calculated. Considering the small difference of these averaged $r_{M\text{-}H}$ distances it is unlikely that a particularly long metal bound-water distance is responsible for the low relaxivity observed for the Mn(II) complex of 1,4-DO2A.

A rough estimation of the relative stability of the [Mn(1,4-DO2A)(H_2O)] and [Mn(1,4-DO2A)] species was made by calculating the free energy variation for the reaction given by:

$$[Mn(1,4\text{-}DO2A)] + H_2O \leftrightarrows [Mn(1,4\text{-}DO2A)(H_2O)] \quad (2)$$

We obtained a value of −0.40 kcal mol^{-1}, which changes to +1.98 kcal ·mol^{-1} upon inclusion of the standard state correction.[45] This result must be taken with care due to the known trend of DFT calculations to favor lower coordination numbers,[46] as well as by the limitations of the PCM model to account for specific solvent−solute interactions, particularly for charged solutes.[47] However, our calculations suggest that the free energy difference between the [Mn(1,4-DO2A)(H_2O)] and [Mn(1,4-DO2A)] species may be relatively small, and therefore the presence of the two species in aqueous solution with different hydration numbers may be responsible for the observed relaxivity.

Variable Temperature NMRD and ^{17}O NMR Measurements. The increase of the longitudinal (R_1) relaxation rate of the water proton spins is predominantly the result of the modulation of the dipolar interaction between the electron (metal-based) and nuclear (of the bound water molecules) magnetic moments. The modulation occurs through rotation of the complex (τ_R), electron magnetic moment relaxation ($T_{1,2e}$), and chemical exchange of the coordinated water molecules with bulk water ($k_{ex} = 1/\tau_M$). The enhancement of R_1 also depends on the number (q) of bound water molecules and their distance ($r_{M\text{-}H}$) from the metal center and on the applied magnetic field strength. Moreover, there is a contribution involving solvent molecules diffusing in the vicinity of the paramagnetic complex (outer-sphere mechanism) that depends on additional param-

dx.doi.org/10.1021/ic302785m | Inorg. Chem. 2013, 52, 3268−3279

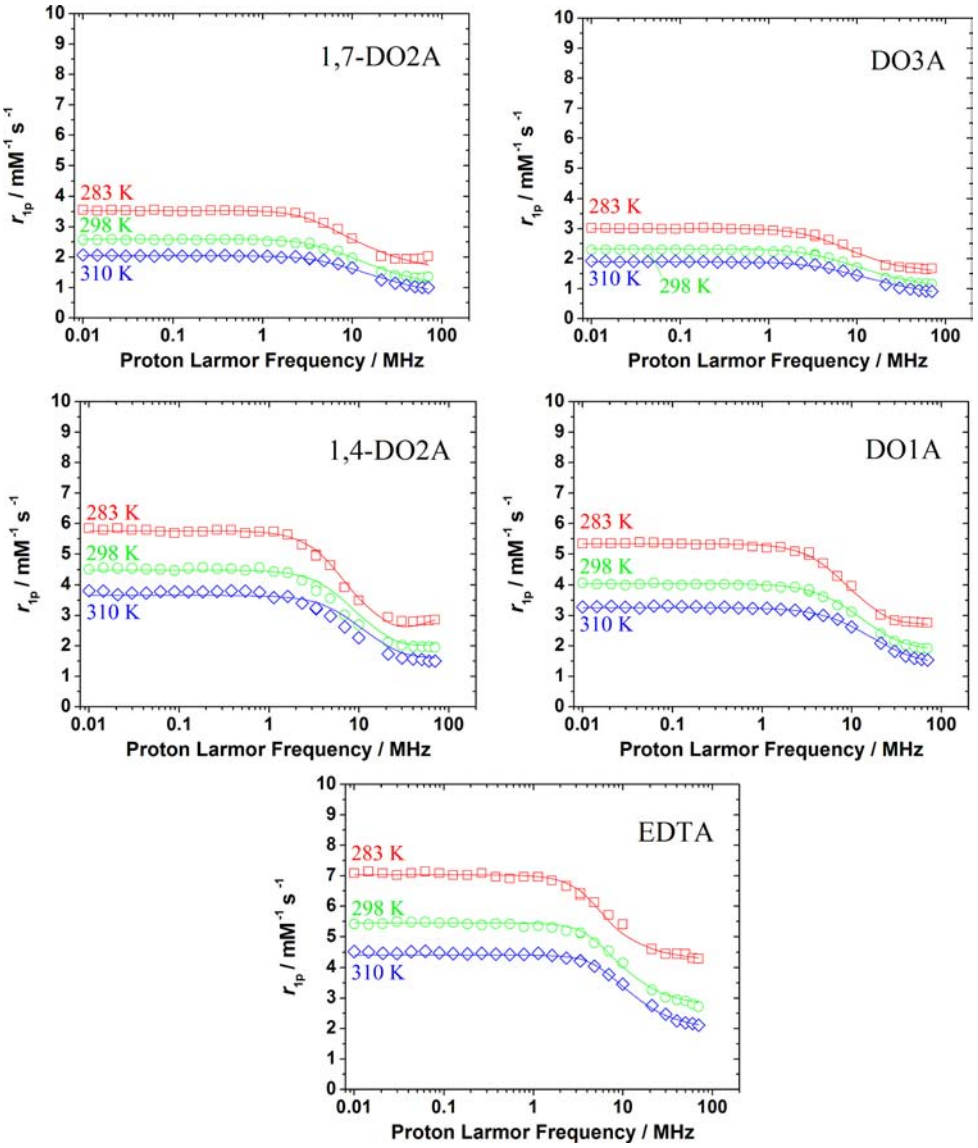

Figure 4. ^{1}H NMRD profiles recorded at different temperatures for the Mn(II) complexes investigated in this work. The lines represent the fit of the data as explained in the text.

eters: the relative diffusion coefficient of solute and solvent molecules, D, and their distance of closest approach, a.

Nuclear magnetic relaxation dispersion (NMRD) profiles of aqueous solutions of [Mn(1,7-DO2A)], [Mn(1,4-DO2A)], [Mn(DO1A)]$^{+}$, [Mn(DO3A)]$^{-}$, and [Mn(EDTA)]$^{2-}$ were measured at 283, 298, and 310 K in the proton Larmor frequency range 0.01−70 MHz, corresponding to magnetic field strengths varying between 2.343×10^{-4} and 1.645 T (Figure 4). As pointed out above, the NMRD profiles recorded for [Mn(1,7-DO2A)] and [Mn(DO3A)]$^{-}$ are consistent with the absence of inner-sphere water molecules coordinated to the metal ion in this complex, the observed relaxivity being the result of the outer-sphere relaxation mechanism. Thus, the NMRD curves were fitted according to the Freed equation[48] for the outer-sphere contribution of the relaxivity. The relaxivity of [Mn(1,4-DO2A)], [Mn(DO1A)]$^{+}$, and [Mn(EDTA)]$^{2-}$ decreases with increasing temperature; this shows that the relaxivity is limited by the fast rotation of the complex in solution, as usually observed for small Mn(II) chelates. Indeed, the shape of the ^{1}H NMRD profiles is typical of low-molecular-weight chelates with a dispersion between 1 and 10 MHz.

In the case of the Mn(II) complex of 1,4-DO2A, DO1A, and EDTA the presence of inner-sphere water molecules results in both inner- and outer-sphere contributions to relaxivity. Therefore, a large set of structural and dynamic parameters affect the observed relaxivity, and thus additional experimental data are required to obtain reliable fittings of the NMRD data. This is often achieved by measuring ^{17}O transverse relaxation rates (R_2) and paramagnetic shifts ($\Delta\omega$) as a function of temperature, typically obtained at a relatively high magnetic field strength (4.7−11.7 T). The temperature dependence of R_2 is given by the Swift−Connick equations,[49] which depend primarily on $T_{1,2e}$, the hyperfine coupling constant $A_O/\hbar$, τ_M, and q. Information on q and $A_O/\hbar$ are also directly accessible from the analysis of the dependence of $\Delta\omega$ with T. The reduced transverse ^{17}O relaxation rates and chemical shifts measured for the Mn(II) complexes of 1,4-DO2A, DO1A, and EDTA are presented in Figure 5.

dx.doi.org/10.1021/ic302785m | Inorg. Chem. 2013, 52, 3268−3279

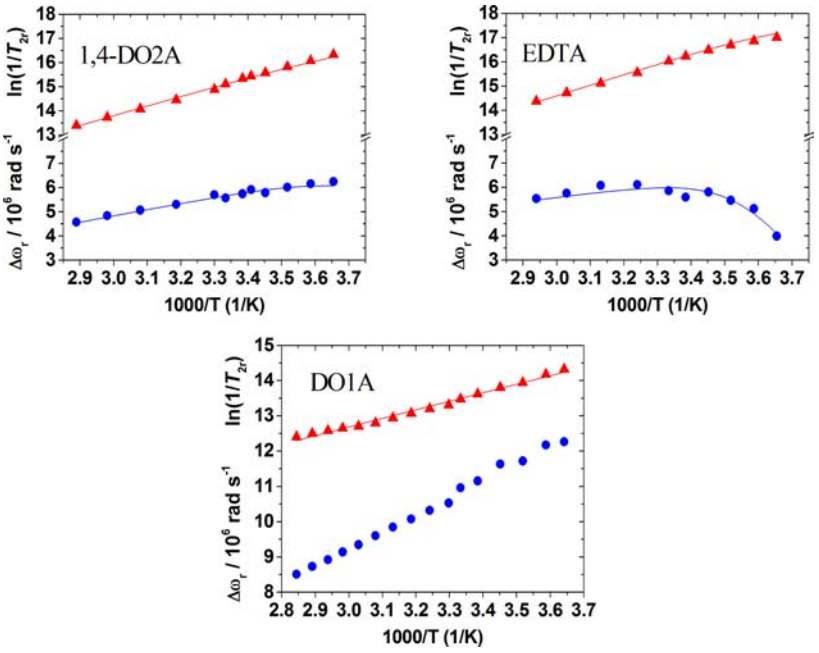

Figure 5. Reduced transverse (red ▲) ^{17}O relaxation rates and ^{17}O chemical shifts (blue ●) for the Mn(II) complexes measured at 11.74 T. The lines represent the fit of the data as explained in the text.

The sign of the temperature dependence of $1/T_{2r}$ depends on whether the transverse relaxation is dominated by τ_M, which decreases with increasing temperature, or by the relaxation time of the bound water molecule, T_{2m}, which normally increases with increasing temperature. For the Mn(II) complexes of 1,4-DO2A, DO1A, and EDTA $1/T_{2r}$ increases with decreasing temperature, which points to a relatively short residence time of the inner-sphere water molecule. However, the changeover between fast and slow exchange limits is clearly observed in the temperature dependence of the chemical shifts of $[Mn(EDTA)]^{2-}$, and to a lower extent in the case of the 1,4-DO2A complex. These qualitative observations indicate that the water exchange rate in $[Mn(EDTA)]^{2-}$ is slower than in the Mn(II) complexes of 1,4-DO2A and DO1A.

Theoretical Calculation of $A_O/\hbar$ and $A_H/\hbar$. In the past decade, methods based on DFT have become an attractive tool for the calculation of hyperfine coupling constants due to the high accuracy that can be achieved at relatively low computational cost. Indeed, DFT calculations have been shown to provide accurate HFCCs for both small organic radicals[50] and d-block transition metal complexes.[51,52] Previous calculations of the hyperfine coupling constants of ^1H and ^{17}O nuclei of inner-sphere water molecules in Gd(III) complexes showed that the computed values depend strongly on the metal−O_W distance.[53] Subsequently, we have recently shown that an accurate computation of hyperfine coupling constants of the inner-sphere water molecule in Gd(III) complexes can only be achieved upon explicit inclusion of a few second-sphere water molecules.[54] Thus, we calculated the ^1H ($A_H/\hbar$) and ^{17}O ($A_O/\hbar$) HFCCs of the coordinated water molecule by using the molecular geometries optimized for the $[Mn(EDTA)(H_2O)]^{2-}\cdot 4H_2O$, $[Mn(1,4\text{-}DO2A)(H_2O)]\cdot 4H_2O$, and $[Mn(DO1A)(H_2O)]^{+}\cdot 4H_2O$ systems at the B3LYP/SVP level (see above). For HFCC calculation purposes we used a basis set of polarized triple-ξ quality for Mn (TZVP) in combination with the EPR-III basis set for C, H, N, and O atoms. The latter basis was especially designed for accurate HFCC calculations of the H, C, and O centers.

Our calculations provide a ^{17}O A_{iso} value of −6.37 MHz for the coordinated water molecule in $[Mn(EDTA)(H_2O)]^{2-}\cdot 4H_2O$, which corresponds to a $A_O/\hbar$ value of 40.0 × 10^6 rad s^{-1}. The latter value is in excellent agreement with that obtained experimentally from ^{17}O NMR data by Hunt and coworkers[55] (A_{iso} = −6.04 MHz, 38.0 × 10^6 rad s^{-1}), and the more recent data reported by van Eldik and coworkers[56] (A_{iso} = −6.4 MHz, 40.2 × 10^6 rad s^{-1}). It is worth noting that in order to fully validate this result it will be useful to extend the study to a number of other complexes. In the case of $[Mn(1,4\text{-}DO2A)(H_2O)]\cdot 4H_2O$ the calculated ^{17}O A_{iso} value amounts to −6.84 MHz, which corresponds to $A_O/\hbar$ = 43.0 × 10^6 rad s^{-1}. A very similar value is obtained for the $[Mn(DO1A)(H_2O)]^{+}\cdot 4H_2O$ system (A_{iso} = −6.27 MHz, $A_O/\hbar$ = 39.4 × 10^6 rad s^{-1}). These calculations therefore indicate that $A_O/\hbar$ is relatively insensitive to the nature of the chelating ligand in this family of complexes, as also observed for different Fe(II) and Ni(II) complexes.[57] This is also in line with the $A_O/\hbar$ values reported in the literature for Mn(II) complexes, which fall within a relatively narrow range ($A_O/\hbar$ = 32 × 10^6 to 40 × 10^6 rad s^{-1}).[5,30−32,42]

The NMRD profiles obtained for $[Mn(H_2O)_6]^{2+}$ and $[Mn_2ENOTA]$ show an unusual dispersion at ca. 0.1 MHz that has been ascribed to an important scalar contribution to ^1H relaxivity. The analysis of the NMRD profiles of these complexes provided absolute values of $A_H/\hbar$ of 2.9 × 10^6 and 4.6 × 10^6 rad s^{-1} for the ENOTA and hexa-aqua complexes, respectively.[31,58] For $[Mn(EDTA)(H_2O)]^{2-}\cdot 4H_2O$, $[Mn(1,4\text{-}DO2A)(H_2O)]\cdot 4H_2O$, and $[Mn(DO1A)(H_2O)]^{+}\cdot 4H_2O$ our calculations provide $A_H/\hbar$ values of −2.0 × 10^6, −1.4 × 10^6, and −3.8 × 10^6 rad·s^{-1}, respectively. There is some lack of clarity about the correct signs of ^1H and ^{17}O HFCCs in Mn(II) complexes. ^{17}O A_{iso} values in Mn(II) complexes are negative, corresponding to positive spin densities at the point nucleus, which leads to high field shifts of the ^{17}O resonance. On the

dx.doi.org/10.1021/ic302785m | Inorg. Chem. 2013, 52, 3268−3279

Table 3. Parameters Obtained from the Simultaneous Analysis of ^{17}O NMR and NMRD Data

	1,7-DO2A	DO3A	1,4-DO2A	EDTA[b]	EDTA[c]	DO1A
$k_{ex}^{298}/10^6$ s^{-1}			1134 ± 64	471 ± 11	471 ± 11	5957 ± 82
$\Delta H^{\ddagger}$/kJ mol^{-1}			29.4 ± 1.7	33.5 ± 0.8	33.5 ± 0.8	17.6 ± 0.4
τ_R^{298}/ps			46 ± 6	57 ± 4	56 ± 4	22 ± 2
E_r/kJ mol^{-1}			19.1 ± 2.6	21.8 ± 2.6	21.8 ± 2.6	20.2 ± 3.8
τ_v^{298}/ps	49 ± 6	18.1 ± 1.6	4.4 ± 0.9	27.9 ± 2.2	27.7 ± 2.2	13.9 ± 1.1
E_v/kJ mol^{-1}	1.3 ± 2.0	6.0 ± 1.4	1.0[a]	1.0[a]	1.0[a]	1.0[a]
$D_{MnH}^{298}/10^{-10}$ m^2 s^{-1}	22.0 ± 0.3	23.5 ± 0.3	23.0[a]	23.1 ± 2.4	22.8 ± 2.4	20.0 ± 0.1
E_{DMnH}/kJ mol^{-1}	19.6 ± 0.4	18.8 ± 0.4	17.3[a]	18.9 ± 3.4	19.2 ± 3.4	17.3 ± 2.4
$\Delta^2/10^{19}$ s^{-2}	2.1 ± 0.3	7.4 ± 0.9	48.1 ± 15.8	6.9 ± 0.7	7.0 ± 0.7	12.8 ± 1.6
$A_O/\hbar/10^6$ rad s^{-1}			43.0[a]	40.5 ± 0.3	40.5 ± 0.3	39.4[a]
$A_H/\hbar/10^6$ rad s^{-1}			0[a]	0[a]	−2.0[a]	0[a]
r_{MnH}/Å			2.83[a]	2.83[a]	2.83[a]	2.83[a]
a_{MnH}/Å	3.6[a]	3.6[a]	3.6[a]	3.6[a]	3.6[a]	3.6[a]
q^{298}	0	0	0.87 ± 0.01	1	1	1
ΔH°[d]/kJ mol^{-1}			−9.3 ± 1.8			
ΔS°[d]/J mol^{-1} K^{-1}			−15.5 ± 6.0			

[a]Parameters fixed during the fitting procedure. [b]Fitted parameters assuming $A_H/\hbar = 0$. [c]Fitted parameters assuming the $A_H/\hbar$ value obtained from DFT calculations (-2×10^6 rad s^{-1}). [d]Thermodynamic data for the hydration equilibrium according to eq 2.

contrary, calculated ^1H A_{iso} values are positive. For $A/\hbar$ we adopt the opposite sign following the criterion used in recent experimental work; therefore, $A_O/\hbar$ values are positive, and $A_H/\hbar$ values are negative. The $A_H/\hbar$ values determined experimentally were obtained from ^1H relaxation measurements, which provide only absolute values. Thus, these experiments did not allow to determine the correct sign of $A_H/\hbar$. As a consequence, both $A_O/\hbar$ and $A_H/\hbar$ were given as positive values, but the theoretical calculations reported here show that they actually have opposite signs.

Simultaneous Fitting of the NMRD and ^{17}O NMR Data. The NMRD profiles obtained for [Mn(1,7-DO2A)] and $[Mn(DO3A)]^-$ could be satisfactorily fitted to the Freed[48] model for outer-sphere relaxation with the parameters listed in Table 3. On the basis of previous studies,[1,4] the distance of closest approach of an outer-sphere water molecule to the paramagnetic center was fixed to 3.6 Å. The values obtained for the diffusion coefficient, D_{MnH}^{298}, and its activation energy, E_{DMnH}, are close to those for self-diffusion of water molecules in pure water: $D_{MnH}^{298} = 2.3 \times 10^{-9}$ m^2 s^{-1} and $E_{DMnH} = 17.3$ kJ mol^{-1},[59] indicating that they are dominated by the rapid diffusion of water molecules.

A simultaneous fitting of the NMRD and ^{17}O NMR data of $[Mn(EDTA)(H_2O)]^{2-}$ was performed with the sets of equations given in the Supporting Information. Some parameters were fixed during the fitting procedure: the distance of closest approach for the outer-sphere contribution a_{GdH} was fixed at 3.6 Å, while the distance between the proton nuclei of the coordinated water molecule and the Mn^{II} ion (r_{MnH}) was fixed at 2.83 Å. The parameters obtained from the fittings are listed in Table 3, while the fitted curves are shown in Figures 4 and 5. The analysis of the NMRD and ^{17}O NMR data of the EDTA complex assuming $A_H/\hbar = -2.0 \times 10^6$ rad s^{-1} did not improve the quality of the fitting, and provided essentially the same parameters obtained with $A_H/\hbar = 0$ (Table 3). Thus, the scalar contribution to relaxivity can be safely neglected in this case.

The ^{17}O NMR chemical shifts obtained for $[Mn(DO1A)(H_2O)]^+$ are considerably larger than those measured for the EDTA and 1,4-DO2A analogues (Figure 5). Several sets of measurements carried out under different concentrations and conditions provided identical results within experimental error. These chemical shifts could be only fitted by using very high $A_O/\hbar$ values (ca. 70×10^6 rad s^{-1}). Such a high hyperfine coupling constant falls well out of the range observed for the Mn(II) complexes investigated up to date, and it also represents about twice the value estimated using our DFT calculations (39.4×10^6 rad s^{-1}, see above). Although we could not find a convincing explanation for this behavior, we believe that such large $A_O/\hbar$ value is unrealistic, and therefore we did not use the ^{17}O chemical shifts for fitting purposes. Instead, only the NMRD profiles and ^{17}O relaxation rates were fitted, with $A_O/\hbar$ fixed to the value obtained from DFT calculations.

A first analysis of the $1/T_1$ NMRD profiles recorded for [Mn(1,4-DO2A)] was performed assuming metal bound-water distances in the order of $r_{M\text{-}H} = 2.75-2.85$ Å, as these appeared to be reasonable distances considering the size of Mn(II) metal ion and coherent with previously reported values for Mn(II) complexes, as well as with our DFT calculations. The best fit of the experimental data on the Bloembergen−Morgan−Freed model would lead to a set of microscopic physical values requiring fractional first sphere hydration level compatible with reasonable electronic relaxation parameters. However, a hydration equilibrium such as the one expressed in eq 2 is expected to be temperature-dependent, and indeed different studies performed on Gd(III) complexes showed that increasing the temperature shifts the equilibrium toward the species with lower hydration number as a consequence of the entropy contribution.[60,61] Unfortunately, attempts to fit the NMRD and ^{17}O NMR data recorded for [Mn(1,4-DO2A)] by leaving q and its temperature dependence as fitting parameters failed. This is a problem associated with the fact that both ^{17}O transverse relaxation rates and paramagnetic shifts depend on q and $A_O/\hbar$, which are directly correlated. Thus, it is not possible to obtain reliable fits of the experimental data using both q and $A_O/\hbar$ as fitting parameters. To overcome this problem, we fixed $A_O/\hbar$ to the value obtained from DFT calculations (43.0×10^6 rad s^{-1}), and introduced q, as well as its temperature dependence given by ΔH° and ΔS° for reaction 1, as fitting parameters. Additionally, the diffusion coefficient, D_{MnH}^{298}, and its activation energy, E_{DMnH}, were fixed to the values determined for self-diffusion of water molecules in pure water.

dx.doi.org/10.1021/ic302785m | Inorg. Chem. 2013, 52, 3268−3279

The analysis of the NMRD and ^{17}O NMR data of [Mn(1,4-DO2A)] confirm the presence of an equilibrium in solution involving a six-coordinate species with $q = 0$ and a seven-coordinate form with $q = 1$. The $\Delta H°$ and $\Delta S°$ values obtained correspond to a q^{298} value of 0.87. As expected, the abundance of the species with lower hydration number increases with temperature as a consequence of the negative $\Delta S°$ value, with the calculated q value changing from 0.90 at 274 K to 0.79 at 346 K.

The τ_R^{298} values obtained from the analysis of the ^1H NMRD profiles are very similar to those reported for small Mn(II) complexes. The lower τ_R^{298} value obtained for the complex of DO1A (22 ps) is in line with the lower molecular weight of this complex in comparison to the DO2A and EDTA analogues.

The water exchange rate determined for $[Mn(H_2O)]^{2+}$ ($k_{ex}^{298} = 2.1 \times 10^7$ s^{-1})[62] is often considerably increased upon complexation, which results in water exchange rates ranging from 5.5×10^7 s^{-1} for Mn(II)-ENOTA to 3.0×10^9 s^{-1} for 12-py-N_4A.[30,31] The water exchange rate constant calculated for [Mn(1,4-DO2A)] is considerably higher than that determined for the EDTA complex, and approaches the value determined for $[Mn(12\text{-py-}N_4A)]^+$. For $[Mn(DO1A)]^+$ the water exchange rate is about 2 times higher than for $[Mn(12\text{-py-}N_4A)]^+$, and the highest water exchange ever measured for a Mn(II) complex. In the case of [Mn(1,4-DO2A)] the fast water exchange rate may be attributed to the presence of a hydration equilibrium involving $q = 0$ and $q = 1$ species, and the similar arrangement of the ligand in these two species (Figure 3). Indeed, the water exchange process in the heptacoordinated $q = 1$ species is expected to proceed following a dissociative mechanism through a six-coordinated transition state. The presence of a hydration equilibrium such as the one expressed in eq 2, and the similar conformation of the ligand in the two forms, implies that the heptacoordinated species has to invest little energy to reach the transition state, which results in a fast water exchange reaction. This reasoning suggests that the water exchange reaction in $[Mn(1,4\text{-DO2A})(H_2O)]$ might involve the six-coordinate [Mn(1,4-DO2A)] species as a reaction intermediate.

ESR Data. The X-band ESR spectra of the Mn(II) complexes of the cyclen-based ligands were recorded at 298 K (center field 0.33 T; Supporting Information). With the exception of [Mn(1,7-DO2A)], the X-band line width values (G) are rather similar with a mean value of 670 ± 60 G: $[Mn(DO1A)]^+$ 738 G, [Mn(1,4-DO2A)] 615 G, and $[Mn(DO3A)]^-$ 678 G. However, the ESR signal of [Mn(1,7-DO2A)] was found to be sensibly larger, 1022 G, under identical experimental conditions. This finding is surprising. One would expect the more symmetrical six-coordinated complexes [Mn(1,7-DO2A)] and $[Mn(DO3A)]^-$ to show narrower ESR signals than the less symmetrical seven-coordinated compounds $[Mn(DO1A)(H_2O)]^+$ and $[Mn(1,4\text{-DO2A})(H_2O)]$. The transverse electron spin relaxation times, T_{2e}, estimated from ESR increase from 64 ps ([Mn(1,7-DO2A)]) to 107 ps ($[Mn(1,4\text{-DO2A})(H_2O)]$, see Supporting Information).

Electron spin relaxation from ESR can be compared to $1/T_{1e}$ and $1/T_{2e}$ from NMR relaxation. ^1H NMR relaxation of inner-sphere water is generally treated using Solomon−Bloembergen−Morgan[63] theory which assumes a transient zero-field splitting (ZFS) mechanism for electron spin relaxation.[64] This approach can be questionable in case of seven-coordinated compounds with low symmetry. In the absence of inner-sphere water ^1H NMR relaxation of solvent water, is described by a dipolar interaction modulated by translational diffusion and electron spin relaxation.[48,65] In our treatment we used the Freed-model together with the Morgan equations for electron spin relaxation (Supporting Information). Transverse electron spin relaxation times T_{2e} calculated at 0.33 T from parameters in Table 3 are of the same order of magnitude (80−180 ps, Table S2) as those calculated from ESR, except for [Mn(1,7-DO2A)] (420 ps). The agreement between NMR and ESR data is therefore quite satisfactory except for [Mn(1,7-DO2A)]. A more detailed discussion of electron spin relaxation would need more experimental data as for example ESR at higher magnetic fields and variable temperature as well as the extension of NMRD profiles to higher Larmor frequencies.

CONCLUSIONS

In this Article, we have addressed a systematic study of the ^1H and ^{17}O NMR relaxometric properties of Mn(II) complexes with a homogeneous series of ligands based on cyclen with denticity 5, 6, and 7. These macrocyclic chelators impose to the metal ion a well-defined coordination geometry, dictated by the typical conformation of the four ethylenediamine moieties of cyclen. However, the results obtained do not show a clear predominance of the coordination number (CN) seven for Mn(II) complexes, as in the case of the EDTA complex, but rather a more complicated behavior in aqueous media involving equilibria between species with different hydration states and consequently coordination number. In fact, DO1A is a pentadentate ligand that forms six-coordinate Mn(II) complexes characterized by the presence of one coordinated water molecule. DO3A is heptadentate, and its Mn(II) complex does not have inner sphere water molecules ($q = 0$); therefore, the metal ion is most likely seven-coordinate. The hexadentate DO2A ligand has two isomeric forms, 1,7-DO2A and 1,4-DO2A, where the Mn(II) complex of the former is predominantly six-coordinate ($q = 0$), but there is evidence of the presence in solution of a seven-coordinate ($q = 1$) minor species that influences to some extent the observed relaxivity over a wide range of magnetic field strength (NMRD profile). On the other hand, in aqueous solutions of [Mn(1,4-DO2A)] the species with one coordinated water molecule ($q = 1$) prevails largely, whereas the $q = 0$ form represents only about 10% of the overall population. Support of presence in solution of species with different states of hydration comes from DFT calculations that indicate a small energy difference between the two isomeric forms. Furthermore, it should be noted that these results confirm the presence of mixtures of complex species with different hydration numbers in the series of Mn(II) complexes with hexadentate ligands derived from AAZ3A, as previously proposed.[5]

In conclusion, aiming at the development of efficient systems based on Mn(II) as an alternative to Gd-based MRI diagnostic probes, a more systematic and thorough study seems necessary to access complexes of improved thermodynamic stability combining a seven-coordinate ground state with one water molecule in the inner coordination sphere under a fast exchange regime.

ASSOCIATED CONTENT

Supporting Information

Equations used for the analysis of the NMRD and ^{17}O NMR data, ESR spectra, comparison of T_{2e} values calculated from ESR line width and NMRD profiles, comparison between

dx.doi.org/10.1021/ic302785m | Inorg. Chem. 2013, 52, 3268−3279

experimental and calculated bond distances for [Mn(EDTA)-$(H_2O)]^{2-}$, and optimized Cartesian coordinates (B3LYP) for the systems investigated in this work. This material is available free of charge via the Internet at http://pubs.acs.org.

AUTHOR INFORMATION

Corresponding Author

*E-mail: mauro.botta@unipmn.it.

Notes

The authors declare no competing financial interest.

ACKNOWLEDGMENTS

C.P.-I. is indebted to Centro de Supercomputación de Galicia (CESGA) for providing the computer facilities. M.B. and L.T. gratefully acknowledge financial support from MIUR (PRIN 2009- C61J11000110001). This work was carried out under the auspices of COST Action TD1004 "Theranostics Imaging and Therapy: An Action To Develop Novel Nanosized Systems For Imaging-Guided Drug Delivery".

REFERENCES

(1) For recent reviews see: (a) Terreno, E.; Delli Castelli, D.; Viale, A.; Aime, S. *Chem. Rev.* **2010**, *110*, 3019−3042. (b) Kubicek, V.; Toth, E. *Adv. Inorg. Chem.* **2009**, *61*, 63−129. (c) Aime, S.; Delli Castelli, D.; Geninatti Crich, S.; Gianolio, E.; Terreno, E. *Acc. Chem. Res.* **2009**, *42*, 822−831. (d) Datta, A.; Raymond, K. N. *Acc. Chem. Res.* **2009**, *42*, 938−947. (e) Dorazio, S. J.; Morrow, J. R. *Eur. J. Inorg. Chem.* **2012**, 2006−2014.

(2) (a) Kueny-Stotz, M.; Garofalo, A.; Felder-Flesch. *Eur. J. Inorg. Chem.* **2012**, *12*, 1987−2005. (b) Drahos, B.; Lukes, I.; Toth, E. *Eur. J. Inorg. Chem.* **2012**, *12*, 1975−1986.

(3) Thomsen, H. S.; Morcos, S. K.; Almen, T.; Bellin, M. F.; Bertolotto, M.; Bongartz, G.; Clement, O.; Leander, P.; Heinz-Peer, G.; Reimer, P.; Stacul, F.; van der Molen, A.; Webb, J. A. W. *Eur. Radiol.* **2013**, *23*, 307−318.

(4) Caravan, P.; Ellison, J.; McMurry, T.; Lauffer, R. *Chem. Rev.* **1999**, *99*, 2293−2352.

(5) Tei, L.; Gugliotta, G.; Fekete, M.; Kalman, F. K.; Botta, M. *Dalton Trans.* **2011**, *40*, 2025−2032.

(6) Bianchi, A.; Calabi, L.; Giorgi, C.; Losi, P.; Mariani, P.; Palano, D.; Paoli, P.; Rossi, P.; Valtancoli, B. *J. Chem. Soc., Dalton Trans.* **2001**, 917−922.

(7) Wang, S.; Westmoreland, T. D. *Inorg. Chem.* **2009**, *48*, 719−727.

(8) Yerly, F.; Dunand, F. A.; Toth, E.; Figueirinha, A.; Kovacs, Z.; Sherry, A. D.; Geraldes, C. F. G. C.; Merbach, A. E. *Eur. J. Inorg. Chem.* **2000**, 1001−1006.

(9) Zetter, M. S.; Grant, M. W.; Wood, E. J.; Dodgen, H. W.; Hunt, J. P. *Inorg. Chem.* **1972**, *11*, 2701−2706.

(10) Meunier, I.; Mishra, A. K.; Hanquet, B.; Cocolios, P.; Guilard, R. *Can. J. Chem.* **1995**, *73*, 685−695.

(11) (a) Li, C.; Wong, W.-T. *J. Org. Chem.* **2003**, *68*, 2956. (b) Kovacs, Z.; Sherry, A. D. *J. Chem. Soc., Chem. Commun.* **1995**, 185−186.

(12) Palsson, L.-O.; Pal, R.; Murray, B. S.; Parker, D.; Beeby, A. *Dalton Trans.* **2007**, 5726−5734.

(13) (a) Dadabhoy, A.; Faulkner, S.; Sammes, P. G.; Long, J. *Chem. Soc., Perkin Trans. 2* **2002**, *2*, 348−357. (b) Barnes, L. S.; Kaneshige, K. R.; Strong, J. S.; Tan, K.; von Bremen, H. F.; Mogul, R. *J. Inorg. Biochem.* **2011**, 1580−1588.

(14) Corsi, D. M.; Platas-Iglesias, C.; van Bekkum, H.; Peters, J. A. *Magn. Reson. Chem.* **2001**, *39*, 723−726.

(15) Becke, A. D. *J. Chem. Phys.* **1993**, *98*, 5648−5652.

(16) Lee, C.; Yang, W.; Parr, R. G. *Phys. Rev. B* **1988**, *37*, 785−789.

(17) Frisch, M. J.; Trucks, G. W.; Schlegel, H. B.; Scuseria, G. E.; Robb, M. A.; Cheeseman, J. R.; Scalmani, G.; Barone, V.; Mennucci, B.; Petersson, G. A.; Nakatsuji, H.; Caricato, M.; Li, X.; Hratchian, H. P.; Izmaylov, A. F.; Bloino, J.; Zheng, G.; Sonnenberg, J. L.; Hada, M.; Ehara, M.; Toyota, K.; Fukuda, R.; Hasegawa, J.; Ishida, M.; Nakajima, T.; Honda, Y.; Kitao, O.; Nakai, H.; Vreven, T.; Montgomery, J. A., Jr.; Peralta, J. E.; Ogliaro, F.; Bearpark, M.; Heyd, J. J.; Brothers, E.; Kudin, K. N.; Staroverov, V. N.; Kobayashi, R.; Normand, J.; Raghavachari, K.; Rendell, A.; Burant, J. C.; Iyengar, S. S.; Tomasi, J.; Cossi, M.; Rega, N.; Millam, N. J.; Klene, M.; Knox, J. E.; Cross, J. B.; Bakken, V.; Adamo, C.; Jaramillo, J.; Gomperts, R.; Stratmann, R. E.; Yazyev, O.; Austin, A. J.; Cammi, R.; Pomelli, C.; Ochterski, J. W.; Martin, R. L.; Morokuma, K.; Zakrzewski, V. G.; Voth, G. A.; Salvador, P.; Dannenberg, J. J.; Dapprich, S.; Daniels, A. D.; Farkas, Ö.; Foresman, J. B.; Ortiz, J. V.; Cioslowski, J.; Fox, D. J. *Gaussian09, Revision A02*; Gaussian, Inc.: Wallingford, CT, 2009.

(18) Schaefer, A.; Horn, H.; Ahlrichs, R. *J. Chem. Phys.* **1992**, *97*, 2571−2577.

(19) Stanton, J. F.; Gauss, J. *Adv. Chem. Phys.* **2003**, *125*, 101−146.

(20) Montoya, A.; Truong, T. N.; Sarofim, A. F. *J. Phys. Chem. A* **2000**, *124*, 6108−6110.

(21) Tomasi, J.; Mennucci, B.; Cammi, R. *Chem. Rev.* **2005**, *105*, 2999−3093.

(22) Schaefer, A.; Huber, C.; Ahlrichs, R. *J. Chem. Phys.* **1994**, *100*, 5829−5835.

(23) Rega, N.; Cossi, M.; Barone, V. J. *J. Chem. Phys.* **1996**, *105*, 11060−11067.

(24) Neese, F. *Coord. Chem. Rev.* **2009**, *253*, 526−563.

(25) Lauffer, R. B. *Chem. Rev.* **1987**, *87*, 901−927.

(26) Aime, S.; Anelli, P. L.; Botta, M.; Brochetta, M.; Canton, S.; Fedeli, F.; Gianolio, E.; Terreno, E. *Biol. Inorg. Chem.* **2002**, *7*, 58−67.

(27) Martell, A. E.; Smith, R. M. *Critical Stability Constants*; Plenum Press: New York, 1974−1989; Vols. *1*−*6*.

(28) Troughton, J. S.; Greenfield, M. T.; Greenwood, J. M.; Dumas, S.; Wiethoff, A. J.; Wang, J.; Spiller, M.; McMurry, T. J.; Caravan, P. *Inorg. Chem.* **2004**, *43*, 6313−6323.

(29) Rolla, G. A.; Tei, L.; Fekete, M.; Arena, F.; Gianolio, E.; Botta, M. *Bioorg. Med. Chem.* **2011**, *19*, 1115−1122.

(30) Drahos, B.; Kotek, J.; Cisarova, I.; Hermann, P.; Helm, L.; Lukes, I.; Toth, E. *Inorg. Chem.* **2011**, *50*, 12785−12801.

(31) Balogh, E.; He, Z.; Hsieh, W.; Liu, S.; Toth, E. *Inorg. Chem.* **2007**, *46*, 238−250.

(32) Drahos, B.; Pniok, M.; Havlickova, J.; Kotek, J.; Cisarova, I.; Hermann, P.; Lukes, I.; Toth, E. *Dalton Trans.* **2011**, *40*, 10131−10146.

(33) Bu, X.-H.; Chen, W.; Mu, L.-J.; Zhang, Z.-H.; Zhang, R.-H.; Clifford, T. *Polyhedron* **2000**, *19*, 2095−2100.

(34) Yang, C.-T.; Li, Y.; Liu, S. *Inorg. Chem.* **2007**, *46*, 8988−8997.

(35) Corey, E. J.; Bailar, J. C., Jr. *J. Am. Chem. Soc.* **1959**, *81*, 2620−2629.

(36) Beattie, J. K. *Acc. Chem. Res.* **1971**, *4*, 253−259.

(37) Valgo, E.; He, Z.; Hsieh, W.; Liu, S.; Toth, E. *Inorg. Chem.* **2007**, *46*, 238−250.

(38) Chen, Z.; Li, Y.; Jiang, C.; Liang, F.; Song, Y. *Dalton Trans.* **2009**, 5290−5299.

(39) Tei, L.; Blake, A. J.; Wilson, C.; Schroder, M. *J. Chem. Soc., Dalton Trans.* **2002**, 1247−1249.

(40) Piguet, C.; Bünzli, J.-C. G.; Bernardinelli, G.; Bochet, C. G.; Froidevaux, P. *J. Chem. Soc., Dalton Trans.* **1995**, 83−97.

(41) Arulsamy, N.; Glerup, J.; Hodgson, D. J. *Inorg. Chem.* **1994**, *33*, 3043−3050.

(42) Drahos, B.; Kotek, J.; Hermann, P.; Lukes, I.; Toth, E. *Inorg. Chem.* **2010**, *49*, 3224−3238.

(43) (a) Wang, X. F.; Gao, J.; Wang, J.; Zhang, Zh. H.; Wang, Y. F.; Chen, L. J.; Sun, W.; Zhang, X. D. *J. Struct. Chem.* **2008**, *49*, 724−731. (b) Gudasi, K. B.; Patil, S. A.; Vadavi, R. S.; Shenoy, R. V.; Nethaji, M.; Bligh, S. W. A. *Inorg. Chim. Acta* **2006**, *359*, 3229−3236.

(44) Mato-Iglesias, M.; Balogh, E.; Platas-Iglesias, C.; Toth, E.; de Blas, A.; Rodríguez-Blas, T. *Dalton Trans.* **2006**, 5404−5415.

(45) Bryantsev, V. S.; Diallo, M. S.; Goddard, W. A., III. *J. Phys. Chem. B* **2008**, *112*, 9709−9719.

(46) Rotzinger, F. P. *Chem. Rev.* **2005**, *105*, 2003−2037.

(47) (a) Bryantsev, V. S.; Diallo, M. S.; Goddard, W. A., III. *J. Phys. Chem. A* **2009**, *113*, 9559−9567. (b) Gutowski, K. E.; Dixon, D. A. *J. Phys. Chem. A* **2006**, *110*, 8840−8856.
(48) Freed, J. P. H. *J. Chem. Phys.* **1978**, *68*, 4034−4037.
(49) (a) Swift, T. J.; Connick, R. E. *J. Chem. Phys.* **1962**, *37*, 307−3020. (b) Swift, T. J.; Connick, R. E. *J. Chem. Phys.* **1964**, *41*, 2553−2554.
(50) Barone, V.; Cimino, P.; Pedone, A. *Magn. Reson. Chem.* **2010**, *48*, S11−S22.
(51) Saladino, A. C.; Larsen, S. C. *Catal. Today* **2005**, *105*, 122−133.
(52) Kossmann, S.; Kirchner, B.; Neese, F. *Mol. Phys.* **2007**, *105*, 2049−2071.
(53) (a) Yazyev, O. V.; Helm, L.; Malkin, V. G.; Malkina, O. L. *J. Phys. Chem. A* **2005**, *109*, 10997−11005. (b) Yazyev, O. V.; Helm, L. *J. Chem. Phys.* **2007**, *127*, 084506_1−084506_8.
(54) Esteban-Gomez, D.; de Blas, A.; Rodríguez-Blas, T.; Helm, L.; Platas-Iglesias, C. *ChemPhysChem* **2012**, *13*, 3640−3650.
(55) Zetter, M. S.; Grant, M. W.; Wood, E. J.; Dodgen, H. W.; Hunt, J. P. *Inorg. Chem.* **1972**, *11*, 2701−2706.
(56) Maigut, J.; Meier, R.; Zahl, A.; van Eldik, R. *J. Am. Chem. Soc.* **2008**, *130*, 14556−14569.
(57) Maigut, J.; Meier, R.; Zahl, A.; van Eldik, R. *Inorg. Chem.* **2008**, *47*, 5702−5719.
(58) Bertini, I.; Briganti, F.; Xia, Z.; Luchinat, C. *Magn. Reson. Imaging* **1993**, *101*, 198−201.
(59) Mills, R. *J. Phys. Chem.* **1973**, *77*, 685−688.
(60) Graeppi, N.; Powell, D. H.; Laurenczy, G.; Zékány, L.; Merbach, A. E. *Inorg. Chim. Acta* **1995**, *235*, 311−326.
(61) Balogh, E.; Mato-Iglesias, M.; Platas-Iglesias, C.; Tóth, É.; Djanashvili, K.; Peters, J. A.; de Blas, A.; Rodríguez-Blas, T. *Inorg. Chem.* **2006**, *45*, 8719−8728.
(62) Ducommun, Y.; Newmannm, K. E.; Merbach, A. E. *Inorg. Chem.* **1980**, *19*, 3696−3703.
(63) Bloembergen, N.; Morgan, L. O. *J. Chem. Phys.* **1961**, *34*, 842.
(64) Helm, L. *Prog. Nucl. Magn. Reson. Spectrosc.* **2006**, *49*, 45−64.
(65) (a) Ayant, Y.; Belorizky, E.; Alizon, J.; Gallice, J. *J. Phys. (Paris)* **1975**, *36*, 991−1004. (b) Fries, H.; Gateau, C.; Mazzanti, M. *J. Am. Chem. Soc.* **2005**, *127*, 15801−15814.